Antibody Recognition of a Flexible Epitope at the DNA Binding Site of the Human Papillomavirus Transcriptional Regulator E2[†]

María Laura Cerutti, Diego U. Ferreiro,[‡] Santiago Sanguineti, Fernando A. Goldbaum,* and Gonzalo de Prat-Gay*

Fundación Instituto Leloir, Consejo Nacional de Investigaciones Científicas y Técnicas, Buenos Aires, Argentina

Received July 28, 2006; Revised Manuscript Received October 27, 2006

ABSTRACT: We have obtained a monoclonal antibody (ED15) against the C-terminal DNA-binding domain of the high-risk human papillomavirus strain-16 E2 protein that strongly interferes with its DNA-binding activity. We here characterize the recognition mechanism of this antibody and find that the ED15−E2 interaction has a strong electrostatic component, which correlates with the high proportion of acidic residues found in the antibody combining site. Further circular dichroism experiments in the presence of phosphate show that, in addition to electrostatic screening of key potential interactions, ionic strength affects the conformation of the epitope. In addition, the interaction is strongly modulated by pH, which correlates with the local flexibility of the epitope rather than the presence of pH sensitive residues at the interface. Noticeably, this finding is well correlated with the strong entropic component of the interaction. Site directed mutagenesis indicates that the ED15 epitope involves at least part of the DNA-binding helix of E2, explaining the mAb inhibitory activity. At physiological salt concentrations, the equilibrium dissociation constant of the E2−ED15 interaction is 10^{-7} M and the association rate is 10^4 M^{-1} s^{-1}, at least 1 order of magnitude slower than those generally reported in the most extensively described "nonflexible" antibody−protein interactions, indicating the presence of a slow conformational rearrangement on the antigen as the rate-limiting step. The crucial role of antigen flexibility in antibody−protein recognition is discussed.

Recognition of antigens by antibodies is a fundamental event in the adaptive immune response. In addition, antibody−antigen interactions have been extensively used as model systems of protein−protein interactions. Comprehensive biochemical and crystallographic data on classical models of protein antigens, such as lysozyme and influenza virus neuraminidase, complexed to typical secondary response high affinity monoclonal antibodies have largely contributed to the recognition mechanisms (reviewed in ref *1*). However, since the protein antigens used in these models are known to be relatively rigid, questions regarding the influence of antigen flexibility on antibody recognition are not easily tractable. Given the growing knowledge about systems in which folding is coupled to ligand recognition, local and global folding processes of proteins upon binding are turning out to be at least as representative as "rigid" proteins (*2*, *3*). Possibly, the more remarkable example of this kind of process is found in transcription factors, where the process of local folding and association with DNA are tightly coupled (*4*−*7*). The papillomavirus E2 transcriptional regulator is a DNA-binding protein in which its DNA recognition helix, although formed, is highly dynamic and flexible (*8*−*10*). E2 is the master regulator of gene transcription and viral DNA replication, and its loss of function has been associated with development of cervical carcinomas (*11*, *12*). As other transcriptional regulators, E2 has a modular architecture: the amino-terminal conforms a transcriptional activation domain that is linked by a disordered hinge region to the C-terminal DNA-binding and dimerization domain (E2C).[1] The E2C domain is formed by two identical polypeptide chains folded into a dimeric β-barrel structure (*13*, *14*). Each monomer contributes four β-strands to the single central barrel and two α-helices that protrude away form it. The major α-helix of each monomer inserts into successive major grooves of the DNA-binding site, making direct contacts with specific DNA bases; this helix is thus termed "the recognition helix". The folding mechanism of the high-risk human papillomavirus-16 (HPV16) E2C was extensively characterized (*15*−*17*), and NMR structures of unfolded (*18*), folded (*10*), and DNA complexed states (*19*) were determined. It was previously shown that pH, phosphate, or sodium salts severely affect the folding and stability of E2C (*15*, *17*), highlighting

[†] This work was supported by grants from Fundación Antorchas and the Consejo Nacional de Investigaciones Científicas y Técnicas (CONICET) to F.A.G., and by Wellcome Trust Grant 077355/Z/05/Z and a grant from ANPCyT to G.P.G., M.L.C, D.U.F., and S.S are recipients of a Ph.D. fellowship from Consejo Nacional de Investigaciones Científicas y Técnicas (CONICET). F.A.G. is a Howard Hughes Medical Institute International Research Scholar (2002−2006).

* To whom correspondence should be addressed. E-mail: gpratgay@leloir.org.ar; fgoldbaum@leloir.org.ar. Fundación Instituto Leloir, Av. Patricias Argentinas 435, Buenos Aires (C1405BWE), Argentina. Tel: 54-11-5238-7500. Fax: 54-11-5238-7501.

[‡] Present address: Center for Theoretical Biological Physics and Department of Chemistry and Biochemistry, University of California San Diego, San Diego, CA.

[1] Abbreviations: E2C, E2 transcriptional activator C-terminal DNA-binding domain; HPV16, high-risk human papillomavirus-16; mAb, monoclonal antibody; V_H, heavy chain variable region; V_L, light chain variable region; CDR, complementarity determining region; k_{ass}, association rate constant; k_{diss}, dissociation rate constant; K_D, equilibrium dissociation constant; CD, circular dichroism.

10.1021/bi0615184 CCC: $33.50
Published on Web 12/08/2006

the sensitivity of this particular fold to changes in the protein microenvironment. Moreover, it has been shown that the DNA binding characteristics of E2C are also affected by subtle changes in experimental conditions (*9*, *20*, *21*). Thus, the highly dynamic character of this viral regulatory protein, along with its strong biomedical relevance, make it a suitable model antigen to study the nature of an antibody−protein interaction in which the antigen is denoted by a remarkable plasticity.

We have previously characterized a set of murine monoclonal antibodies (mAb) against the HPV16 E2C domain (*22*). Epitope mapping and functional analysis of the generated anti-E2C mAbs revealed the presence of two separate antibody populations: one formed by antibodies directed against an epitope totally or partially overlapped with the DNA-binding surface of the transcription factor, interfering with E2C binding to DNA; and other which recognize a repetitive epitope on the opposite surface of the dimeric domain, able to form a stable ternary complex with protein and DNA. In the present work we further characterize the interaction of E2C with the DNA-binding inhibitory mAb ED15. An epitope-mapping ELISA assay confirmed that ED15 recognizes an epitope comprising part of the E2C DNA recognition helix, explaining its DNA-binding inhibitory activity (*22*). Amino acid sequence analysis shows that the ED15 paratope is highly acidic, possibly electrostatically complementary to the basic E2C DNA-binding surface. We characterized both the kinetic and thermodynamic parameters of the antibody−antigen interaction by surface plasmon resonance and isothermal titration calorimety and analyzed the antigen secondary structure by circular dichroism spectroscopy. We found that the ED15−E2C interaction is highly electrostatically driven, and that the E2C flexibility plays a critical role in the antibody recognition. Our results show that the ED15−E2C pair is an excellent antibody−protein model to study the nature of the forces driving the humoral immune recognition of flexible and positively charged antigens, as are most nucleic acid regulatory proteins.

EXPERIMENTAL PROCEDURES

E2C Purification, Mutagenesis, and Biotinylation. The C-terminal 80-amino acid DNA-binding domain of the HPV16 E2 wild type and mutant proteins were produced, expressed, and purified as previously described (*23*). Taking into account the high proportion of basic amino acids E2C has in its DNA-binding surface, a kit designed to biotinylate the carboxyl groups of the protein was employed: the EZ-Link Biotin-LC-PEO-Amine kit (Pierce Chemicals, Rockford, IL). Since biotinylation of carboxylic groups is not an efficient chemical reaction, several modifications to the standard protocol had to be made. The final protocol was as follows: 250 μg of E2C (1.5 mg/mL) in 0.1 M MES [(2-*N*-morpholino) ethanesulfonic acid] pH 5.5, 1 mM DTT was incubated with 125 μL of 50 mM Biotin-LC-PEO-Amine and 62.5 μL of 1 mg/mL EDC (1-ethyl-3-[3-dimethylaminopropyl] carboiimide hydrochloride) for 2 h at room temperature with stirring. Reagents in excess were removed by dialysis.

E2C DNA Ligand. The sequence of the double-stranded oligonucleotide used in the isothermal titration calorimetry experiments corresponds to E2 site 35 in the HPV-16 genome. The sequence of the A chain is 5′-GTAACCGAAATCGGTTGA-3′ (HPLC purified, IDT, Coralville, IA). Single stranded oligonucleotide concentration determination and annealing were carried out as described (*23*).

MAbs Purification and Sequencing. MAb ED15 and ED23 IgGs (*22*) and their derived Fab fragments were prepared following standard procedures (*24*). Messenger RNAs from the ED15 and ED23 hybridoma cell lines were extracted and purified using a Fast-track kit (Invitrogen), and cDNA was synthesized using the Copykit (Invitrogen) with an oligo-(dT) primer. Degenerate primers designed for amplification of mouse heavy and light variable region sequences (V_H and V_L, respectively) (*25*) were employed, and the PCR products were cloned using the TA cloning kit (Invitrogen). Several clones for each chain were sequenced to ascertain the absence of artifacts arising from PCR amplification. Complementary determining residues and framework regions were defined according to Kabat (*26*). Where the Kabat definitions of the CDRs differed from Chothia definitions (*27*), the Chothia scheme was followed. The theoretical isoelectric points (p*I*) of the heavy and light variable regions were obtained using the ProtParam program (ExPASy).

ELISA Assays. Maintenance of the ED15 epitope following E2C carboxy-biotinylation was subsequently checked by assaying mAbs reactivities against the labeled protein by ELISA. Briefly, 96-well ELISA plates (Maxisorp, Nunc) were sensitized with 1 μg of streptavidin in Tris buffer saline (TBS) and blocked with 1% bovine serum albumin in TBS. Next, different amounts of biotinylated E2C (10−1000 nM) were incubated for 20 min. In order to avoid nonspecific binding of E2C to the plate, this step was carried out under high ionic strength and reducing conditions (TBS plus 1 M NaCl and 1 mM DTT). Then, 1 μg of purified IgG mAbs or polyclonal anti-E2C antibody sera in blocking solution was added to each well and their reactivities were tested by incubating with peroxidase-conjugated polyclonal antibodies to murine IgG Fc fragment (Accurate, USA). All incubations were performed during 1 h at room temperature. The reaction was developed according to standard procedures, and the final color was read at 492 nm in an ELISA Reader (S960 Metertech Inc., Taiwan).

The epitope mapping ELISA assay was carried out by sensitizing the plate with 0.25 μg/well of E2C or E2C mutants in TBS buffer. After blocking, solid-phase E2C proteins were incubated with purified mAbs IgG (0.5 μg/well in blocking solution). The reaction was developed as described above.

Kinetic Measurements. The kinetics of association and dissociation between the anti-E2C mAbs and E2C were studied in an IAsys plus Affinity Sensor Biosensor (Thermo-Labsystems). E2C coupled to biotin and added to a cuvette previously derivatized with streptavidin was used as the solid-phase ligand in the assay. Streptavidin coupling to the biosensor carboxymethyl dextrane matrix cuvette was carried out using the EDC/NHS coupling kit as recommended by the supplier. Briefly, 4 μg of streptavidin (1 mg/mL) in 10 mM sodium acetate pH 5.6 was added to the cuvette. After coupling, nonreacted NHS ester groups were blocked with 1 M ethanolamine. 200 arc sec response units of streptavidin was obtained after removing loosely associated protein with 10 mM HCl. Then, biotin-labeled E2C was placed in the cuvette and incubated until the signal response

	FR1	CDR1	FR2	CDR2
ED15	EVQLQEESGSELVRSGASVKLSCTASGFNIK	**DYYVH**	WVKQRTEQGLEWIG	**WIDPENGDSECADKNQG**

	FR3	CDR3	FR4
	KATMTADTSSNVAYLHLSSLTSEDTAVYYC	**FSIYYDSTY**	WGQGTTVTVSS

	FR1	CDR1	FR2	CDR2
ED23	EVQLQQSGAELVKPGASVKISCKASG	**YTFTDYIMD**	WMKQSPGKSLEWIG	**NIHPNYDVTSYNQKFKGKATL**

	FR3	CDR3	FR4
	TVDRSSSTAYMELRSLTSEDTALYYCTR	**RVGNFEFTY**	WGQGTL

FIGURE 1: Amino acid sequences of the V_H regions of the ED15 and ED23 anti-E2C mAbs. The framework (FR) and complementarity determining regions (CDR) are indicated above the appropriate sequence segments in the figure.

reached equilibrium. This step was carried out under high ionic strength buffer conditions to avoid protein aggregation on the derivatized surface (25 mM Bis-Tris-HCl pH 7.0, 1 M NaCl, 1 mM DTT). The optimal amount of biotinylated E2C needed to be immobilized for the subsequent kinetic constant measurements was determined by following the binding response upon incubation with different mAbs concentrations. Preliminary experiments revealed that the kinetic and equilibrium parameters obtained using univalent Fab fragments or divalent whole IgG molecules were almost indistinguishable. As the sensorgrams obtained with IgG molecules yielded better signal-to-noise ratio, subsequent experiments were therefore performed with purified IgG mAbs.

Studies of the ionic strength of antibody−E2C kinetic constants were carried out in 25 mM Bis-Tris or 10 mM sodium phosphate buffer pH 7.0 plus 1 mM DTT, and different concentrations of NaCl (65 − 240 mM). The ionic strength of the solutions was calculated as $I = 0.5\sum_i m_i z_i^2$, where m_i are the molarities and z_i are the charges of each of the i species. Kinetic experiments of ED15 binding to E2C at different pHs were carried out in 10 mM sodium phosphate buffer (pH range 5.5 − 8.0), 50 mM NaCl, and 1 mM DTT. In all cases, rate constants for association and dissociation were obtained by globally fitting the data from five to eight injections of different concentrations (10^{-9}−10^{-6} M) of antibody using the Fastplot software (ThermoLabsystems) using the 1:1 Langmuir binding model. In order to minimize artifacts that arose by sample injection, antibody samples were prepared in the same buffer as that contained in the cuvette. All experiments were performed at 25 °C.

Circular Dichroism Spectroscopy. Circular dichroism (CD) spectra were monitored in the far-UV region using J810 equipment (Jasco, Japan). Ten scans were averaged for each measurement at 25 ± 0.1 °C. Data were collected with a scan rate of 100 nm min^{-1} in a 0.1 cm path length cuvette. Studies of the effect of the ionic strength on E2C conformation were performed at a 30 μM protein concentration in 10 mM Bis-Tris or sodium phosphate buffer pH 7.0 with 1 mM DTT, and different concentrations of NaCl (60 − 360 mM). CD spectra of wild type and E2C mutants (10 μM) were measured in 10 mM sodium acetate buffer, pH 5.6 with 1 mM DTT. In all cases, the protein samples were extensively dialyzed in each buffer condition prior to CD measurements.

Isothermal Titration Calorimetry. Experiments were performed using the VP-ITC (MicroCal, USA). Samples were prepared by dialyzing all interacting components extensively into 10 mM sodium phosphate pH 7.0, 178 mM NaCl, and 0.2 mM DTT. In each experiment, the ligand in the cell (9 μM site 35 double-stranded oligonucleotide or 11.5 μM ED15 IgG binding sites) was titrated with several injections of E2C protein (94 μM). The volume of each injection was 8 μL, except for the first injection, which was 2 μL and was subsequently eliminated from data analysis. Injections were continued beyond saturation levels to allow for determination of heats of ligand dilution. After substracting the heat of dilution, the resulting data were fitted to a single-site binding isotherm using the Microcal ORIGIN 5.0 software supplied with the instrument. The antibody binding sites were assumed to be independent, and the concentration of active antibody was therefore adjusted based on a 1:1 stoichiometry of interaction. All measurements were carried out at 298 K.

RESULTS

The V_H Domain of mAb ED15 is Highly Acidic. The primary structure of the anti-E2C mAb ED15 was determined from its cDNA sequence (Figure 1). The amino acid sequence of the heavy chain variable region (V_H) presents a noticeably high proportion of acidic residues (16 out of 116, 13.8%) and a low proportion of basic ones (6 out of 116 residues, 5.2%). In particular, the second complementarity determining region (CDR) presents five negatively charged and only one positively charged residue. Overall, this amino acid pattern gives the ED15 V_H region a theoretical isoelectric point (p*I*) of 4.29 (ExPASy ProtParam (*28*)). On the contrary, the V_H amino acid sequence of ED23, an antibody directed against a continuous epitope on the opposite face of the transcription factor, presents almost the same proportion of acidic and basic residues (11 out of 113 residues, 9.7%, and 12 out of 113 residues, 10.6%, respectively). As a consequence, the calculated p*I* value of this region is ∼8.0. The light chain variable regions (V_L) of both antibodies have p*I*s of 8.60 and 8.39 for ED15 and ED23, respectively.

The E2C−ED15 Interaction Has a Strong Electrostatic Component. Since the highly acidic nature of the ED15 V_H region seems to be electrostatically complementary to the basic surface of the E2 DNA-binding site, we next investigated the role of the electrostatic forces in the formation of this protein−antibody complex. The effect of the ionic strength on the interactions of ED15 and the control mAb ED23 with E2C was investigated by surface plasmon resonance. Initial binding studies were performed in Bis-Tris buffer at pH 7.0, a condition previously used to characterize the interaction of E2C with its target DNA sequences (*23*). Table 1 shows the association (k_{ass}) and dissociation (k_{diss}) rate constants, as well as the equilibrium dissociation constant (K_D) of the ED15−E2C interaction at different NaCl concentrations. At intermediate salt concen-

Table 1: Effect of Ionic Strength on the E2C−mAb Interactions in Bis-Tris Buffer[a]

	ED15			ED23		
ionic strength (mM)	k_{ass} (M^{-1} s^{-1})	k_{diss} (s^{-1})	K_D (M)	k_{ass} (M^{-1} s^{-1})	k_{diss} (s^{-1})	K_D (M)
75	9.54×10^4	7.20×10^{-3}	7.51×10^{-8}	1.03×10^5	5.40×10^{-3}	5.24×10^{-8}
100	7.24×10^4	9.30×10^{-3}	1.29×10^{-7}	1.66×10^5	3.30×10^{-3}	2.01×10^{-8}
125	1.38×10^4	1.21×10^{-2}	8.70×10^{-7}	8.74×10^4	5.60×10^{-3}	6.40×10^{-8}
150	7.31×10^3	9.0×10^{-3}	1.23×10^{-6}	1.40×10^5	4.70×10^{-3}	3.40×10^{-8}
175	1.34×10^3	9.9×10^{-3}	7.39×10^{-6}	8.58×10^4	4.50×10^{-3}	5.21×10^{-8}

[a] Measurements were carried out in 25 mM Bis-Tris buffer pH 7.0, 1 mM DTT and increasing NaCl concentrations. Constant values were obtained by global fitting of data from five to eight different concentrations of antibody (10^{-9}−10^{-6} M) to a 1:1 binding model. The temperature was set at 25 °C. The K_D is calculated as k_{diss}/k_{ass}.

trations, the k_{ass} is around 10^4 M^{-1} s^{-1} and the kinetic off-rate is around 10^{-2} s^{-1}. Increasing the buffer ionic strength from 75 to 175 mM produces a 70-fold reduction in the k_{ass}, without affecting the k_{diss}. Assuming a two state binding model, the calculated K_D drops 2 orders of magnitude within these ionic strength limits, indicating that the ED15 binding is strongly modulated by salt. As a control, the interaction of ED23 with E2C is insensitive to ionic strength changes (Table 1 and Figure 2A, open circles).

Logarithmic representation of the k_{ass} versus the square root of ionic strength shows a linear dependence between these two parameters for the ED15−E2C interaction (Figure 2A, closed circles). Fitting of the data according to a simple

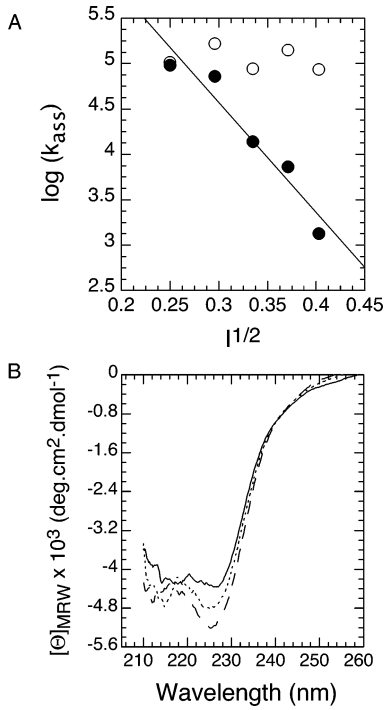

FIGURE 2: Effect of ionic strength on the E2C−mAb interactions in Bis-Tris buffer. (A) Debye−Hückel plot showing the ionic strength dependence of the k_{ass} for the ED15−E2C (closed symbols) and ED23−E2C interactions (open symbols; see legend Table 1 for details). The data were fitted to the Debye−Hückel relationship: $\log k_{ass} = \log k^0_{on} + z_{ag}z_{ab}I^{1/2}$, where k_{ass} is the association rate constant at an ionic strength I, k^0_{on} is the association rate constant at zero ionic strength (by extrapolation), and z_{ag} and z_{ab} are the charges of the antigen and antibody, respectively. (B) Comparison of the far-UV CD spectra of the HPV16 E2C antigen at different ionic strength concentrations. Spectra were recorded in 10 mM Bis-Tris buffer pH 7.0, with 1 mM DTT, at 80 mM (solid line), 160 mM (dotted line), and 360 mM (dashed line) ionic strength at 30 μM protein concentration.

Debye−Hückel model gives a slope of −12 and an extrapolated k_{ass} at 0 ionic strength of 1.6×10^8 M^{-1} s^{-1}. To our surprise, we found that the slope value is well out of the range of those commonly described for protein−protein associations. The higher value reported for a nearly completely electrostatically steered protein−protein complex is that of the thrombin−thrombomodulin interaction, with a slope value of −6 (*29*). Since it has been reported that the folding properties of E2C are sensitive to changes in the ionic strength (*17*), not only may the observed effect be related to the electrostatics of the interaction but also antigen conformational changes could be taking place.

In order to analyze the effect of ionic strength on E2C conformation, we used circular dichroism spectroscopy to evaluate the secondary structure of the protein upon salt addition. The far-UV circular dichroism (CD) spectra of E2C in Bis-Tris buffer presents two distinctive minima at 210 and at 224 nm and a maximum at 195 nm, corresponding to a substantial amount of α-helical contributions (*15*). Figure 2B shows the CD spectra of E2C at different ionic strength concentrations in Bis-Tris buffer. The increment in buffer ionic strength from 80 mM to 360 mM produces a decrease of approximately 1000 deg cm^2 $dmol^{-1}$ in molar ellipticity ($[\Theta]_{MRW}$) at both α-helix minima. It should be noted that the spectra at both high and low ionic strength are indicative of folded ensembles, ruling out unfolding as a possible cause of the weakened ED15 interaction. Furthermore, since the overall folding of the E2C domain is stable at high ionic strength (*17*), we speculate that the observed conformational changes are local, and possibly restricted to the α-helical regions.

Effect of Phosphate Salts on the ED15−E2C Interaction. In order to separate the contribution of the electrostatic forces from the conformational changes induced by salt on E2C, we conducted a new series of spectroscopic and kinetic studies in different experimental conditions. Since it was previously shown that phosphate salts have a strong stabilizing effect on E2C folding, the behavior of the E2C domain under different ionic strength conditions was evaluated in sodium phosphate buffer. Figure 3B shows that the increment in buffer ionic strength produces only a minor change in E2C secondary structure. In particular, small but significative changes (200 deg cm^2 $dmol^{-1}$ in $[\Theta]_{MRW}$) in the 210 and 224 nm bands of the CD spectra are observed when ionic strength is increased from 80 to 360 mM. Thus, the overall domain conformation remains almost unaffected by salt increment in the presence of phosphate salts, the mentioned CD changes likely being related to a stabilizing phosphate effect on the protein (*9*).

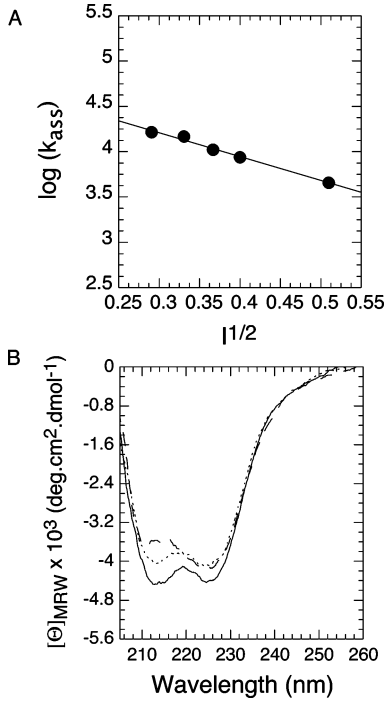

FIGURE 3: Effect of ionic strength on the E2C−ED15 interaction under antigen stabilizing conditions. (A) Debye−Hückel plot representation of the kinetic parameters of the ED15−E2C interaction under different ionic strength conditions in phosphate buffer. (B) Far-UV CD spectra of E2C (30 μM) in 10 mM sodium phosphate buffer pH 7.0, with 1 mM DTT, at 80 mM (solid line), 160 mM (dotted line), and 360 mM (dashed line) ionic strength concentrations.

Table 2: Ionic Strength Dependence of the ED15−E2C Interaction in Phosphate Buffer[a]

ionic strength (mM)	k_{ass} (M^{-1} s^{-1})	k_{diss} (s^{-1})	K_D (M)
85	1.64×10^4	1.09×10^{-3}	6.64×10^{-8}
110	1.47×10^4	1.34×10^{-3}	9.12×10^{-8}
135	1.05×10^4	0.96×10^{-3}	9.14×10^{-8}
160	8.70×10^3	0.91×10^{-3}	1.04×10^{-7}
260	4.50×10^3	1.10×10^{-3}	2.43×10^{-7}

[a] Measurements were carried out in 10 mM sodium phosphate buffer pH 7.0 with 1 mM DTT and increasing concentrations of NaCl.

The effect of ionic strength in the kinetics of binding of ED15 to E2C in phosphate buffer is showed in Table 2. While no changes on the dissociation rate constant are observed (average $k_{diss} = 10^{-3}$ s^{-1}), the k_{ass} displays a 3.5-fold reduction when ionic strength is increased from 85 to 260 mM. Consequently, the K_D is also reduced 3.5-fold within this ionic strength range. The representation of the data in a Debye−Hückel plot is shown in Figure 3A. In this case, the slope of the plot is −2.6, a value that falls within the range of those reported in highly electrostatically steered protein−protein interactions (reviewed in ref *29*). Therefore, the stabilization of the viral domain by phosphate allowed as to establish the electrostatic character of the ED15−E2C interaction. However, the extrapolated k_{ass} value at 0 ionic strength is 3 orders of magnitude smaller than that obtained in the Bis-Tris experiments ($\sim 1 \times 10^5$ M^{-1} s^{-1}), indicating that the thermodynamic stabilization of E2C operates against binding to the antibody (see below).

ED15 Binding to E2C Is Sensitive to pH and Entropically Driven. It was previously shown that pH strongly affects the stability of E2C, changing its unfolding and dissociation equilibrium constants (*15*, *17*). Taking this into account, we subsequently evaluated whether ED15 binding is also modulated by pH. The kinetic parameters of the ED15−E2C interaction measured in a wide pH range in phosphate buffer are shown in Table 3. The k_{ass} increases at acidic pH, being 10-fold faster when the pH goes from 7.0 to 5.5. On the contrary, the dissociation rate constant remains unaffected. As a result, the K_D shows a clear dependence on pH, which decreases 13-fold from pH 7.0 to 5.5 ($\sim 9 \times 10^{-8}$ to $\sim 7 \times 10^{-9}$ M, Figure 4). CD spectra of the E2C domain at these pH conditions are almost superimposable (data not shown). Thus, the sensitivity of the ED15−E2C interaction to pH variations can be ascribed to the interaction itself and not to major local conformational changes on the epitope. No reliable determination of the constants could be attained at pH 5.0, probably due to the marginal stability of the dimer at this pH (*15*, *17*). This result would be indicating that ED15 binding is sensitive to the E2C unfolding that takes place a low pH (<5.5).

Table 3: pH Dependence of the ED15−E2C Kinetic Constants

pH	k_{ass} (M^{-1} s^{-1})	k_{diss} (s^{-1})
5.5	1.44×10^5	1.00×10^{-3}
6.0	5.58×10^4	1.09×10^{-3}
6.5	2.15×10^4	1.15×10^{-3}
7.0	1.24×10^4	1.10×10^{-3}
8.0	1.47×10^4	1.42×10^{-3}

[a] Measurements were carried out in 10 mM sodium phosphate buffer plus 1 mM DTT and 50 mM NaCl.

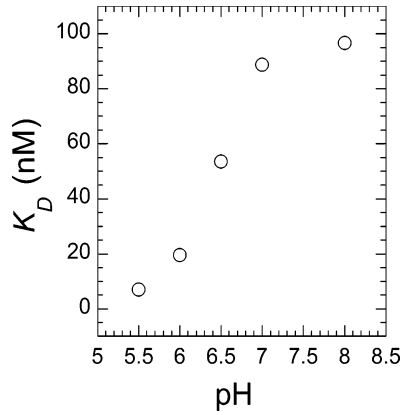

FIGURE 4: Dependence of the ED15−E2C equilibrium dissociation constant on pH. The association and dissociation rate constants were determined at different pH values in sodium phosphate buffer (see Table 3).

In order to investigate the enthalpic/entropic components of the ED15−E2C interaction, we carried out isothermal titration calorimetry (ITC) experiments. Figure 5A shows the raw calorimetric data of the ED15−E2C interaction (upper line). No detectable heat change of binding was observed (Figure 5B, open symbols), even when different ionic strength conditions were assayed (not shown). The binding isotherm for the interaction of E2C with its DNA ligand carried out in identical conditions confirms that the lack of signal in the ED15−E2C interaction is due to a very low ΔH component. The titration curve (Figure 5A, lower trace) shows the steep change in specific heat characteristic for tight binding reactions with a marked enthalpic component, and the calculated ΔH of binding is −21.0 kcal per

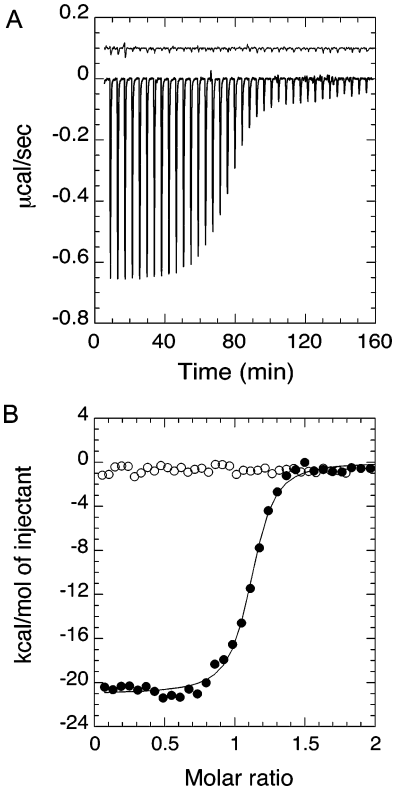

FIGURE 5: The ED15−E2C interaction is entropically driven. (A) Raw data showing the heat released during binding of E2C to ED15 (upper trace) and site 35 (lower trace) in phosphate buffer at 200 mM ionic strength. A factor of 0.1 was added to the ED15−E2C titration data to avoid data overlapping and better visualize the traces. (B) Integrated heat of binding for the E2C−ligand interactions at 298 K. Data for the E2C−ED15 interaction showing no heat change are plotted in open symbols. Data were fitted to a single binding model, assuming an effective concentration of antibody binding sites. As a control, the heat change of the enthalpically driven E2C−DNA interaction is shown in closed symbols.

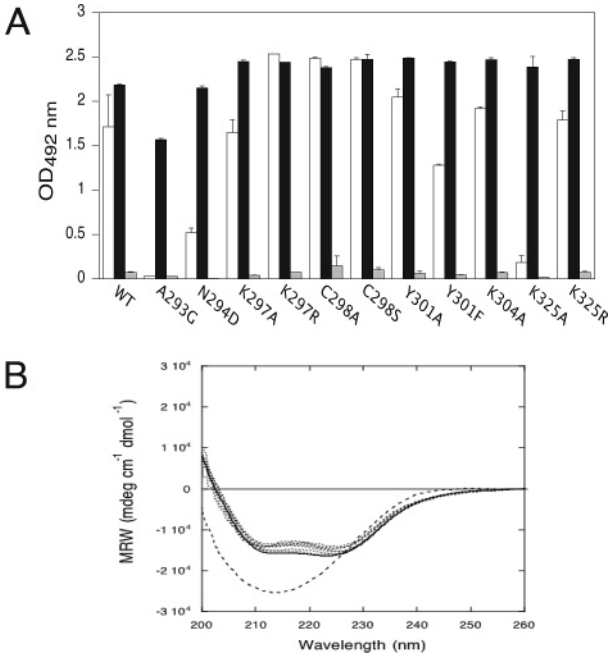

FIGURE 6: MAb ED15 recognizes the highly flexible DNA-binding helix of the E2 transcription factor. (A) ELISA reactivity of ED15 (open bars) ED23 mAbs (closed bars) against a panel of E2C mutants. Single amino acid residue E2C mutants were used as antigen and antibody reactivity was developed as described in Experimental Procedures. Gray bars represent the reactivity of a control mAb. (B) Superimposition of the far UV−CD spectra of the wild type (solid line) and E2C mutants (dotted line) in 10 mM sodium acetate buffer, pH 5.6 with 1 mM DTT. Protein concentration was 10 μM. The spectrum showing an anomalous CD signal corresponds to the N293G mutant.

mole of E2C (Figure 5B, closed symbols). These results indicate that the ΔG of the ED15−E2C interaction must be driven by entropy.

MAb ED15 Recognizes an Epitope in the DNA-Binding Surface of E2C. We have previously shown that ED15 interferes with E2C−DNA complex formation (*22*). However, we had no direct evidence that the epitope recognized by this mAb was located at the DNA-binding surface of the protein. In order to further characterize the epitope recognized by ED15, we carried out a site-directed mutagenesis epitope-mapping approach, in which E2C mutants carrying a single amino acid residue substitution along the DNA-binding surface were used as antigens. Most site directed mutants were shown not to disturb the overall protein structure, which allowed the energetic changes to be assigned to individual side chain group substitution (*30*).

Figure 6A shows the reactivity of mAb ED15 against a panel of single point E2C mutants at the DNA-binding helix, analyzed in an ELISA experiment. Mutation A293G produces a significant decrease in ED15 reactivity. This replacement is located at the N-cap of the helix, and unlike all other mutants, generates a substantial conformational change in E2C, most likely perturbing the entire DNA-binding helix (Figure 6B). Therefore, the decrease in ED15 reactivity against this mutant is more likely to be due to the overall distortion of the epitope rather than the lack of essential contacts with the side chain of the mutated residue. On the other hand, the A293G replacement did not affect the mAb ED23 reactivity, constituting an internal control of the ED15 binding.

Mutations in several exposed residues of the α-helix that do not affect the E2 DNA-binding helix conformation have no effect on ED15 reactivity, suggesting that many of the residues involved in the E2C−DNA interaction are not part of the epitope recognized by this mAb. The residues where the effect on antibody binding is significant and may imply direct contacts are N294D, Y301, located at the N-cap and center of the DNA-binding helix, respectively, and K325, located in the nearby $\beta 2-\beta 3$ loop (residues 321−328. Figure 7). This loop is believed to contact the DNA, since it is located near in space and single mutations affect DNA binding (*19*, *30*). Mutation N294D severely affects ED15 reactivity. In this case, despite the replacement's being made on a residue located at the N-cap of the recognition helix, no changes on E2C conformation were observed (Figure 6B). Thus, the decrease in ED15 reactivity against this mutant may be due either to the loss of a direct interaction with the asparagine side chain or to a repulsive effect of the negative charge of the aspartic residue. Mutation Y301F does not affect binding, indicating that the OH group of Y301 is not involved in direct contacts with the antibody. On the other hand, the substitution Y301A produces a detectable decrease in ED15 reactivity, indicating that this difference can be ascribed to the aromatic motif ring of the tyrosine. Mutation K325A produces a significant decrease in ED15 reactivity, which is completely restored when a conservative replace-

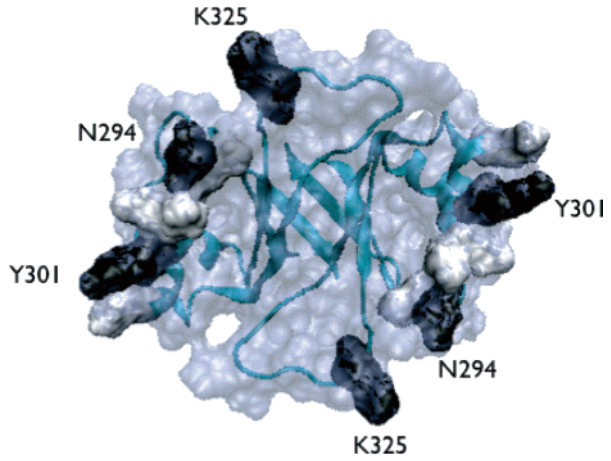

FIGURE 7: Putative recognition site of ED15. The high-resolution structure of the E2C dimer was taken from the protein data bank (pdb id: 1R8P), oriented to show the DNA binding face. The molecular surface was calculated using a 1.4 Å sphere and is represented as a transparent surface. The surface of the mutated residues is shown solid, and colored according to the ED15 reactivity (high in white, low in black). The labels mark the residues that are proposed to be directly involved in ED15 binding. The figure was prepared with VMD (*47*) and the coordinates deposited by Nadra et al. (*10*).

ment to Arg is assayed. This result suggests that a nonspecific electrostatic interaction between E2C and ED15 is taking place. Altogether, these data confirm that ED15 recognizes an epitope located at the DNA-binding surface of the HPV16 transcription factor, explaining its inhibitory activity. In addition, they support that ED15 is extremely sensitive to local perturbations of this epitope.

DISCUSSION

The relevance of plasticity in macromolecular interactions is gaining more attention every day as it allows linking and extending conformational variants to biological function. Among protein−protein interactions, antigen−antibody complexes are one of the systems in which plasticity is more evident. In the last years, many reports have addressed the importance of flexibility in antibody binding, mainly focusing in the precomplexed antibody dynamics (*31*−*36*). Unfortunately, the fact that in these studies haptens or peptides were used as antigens has limited the analysis of the opposite situation, *i.e.*: to what extent does antigen flexibility influence antibody recognition? In order to get insight into this question we carried out a comprehensive study of the interaction of the DNA-binding domain of the HPV16 E2 transcription factor with the specific mAb ED15. We here demonstrated that the mAb recognition is severely affected by the occurrence of conformational changes on the viral protein, the interaction being entropically driven. In addition, we showed that the ED15−E2C interaction has a predominant electrostatic component, being one of the highest electrostatically steered antibody−protein interactions described until the present.

Analysis of the primary sequences of the anti-E2C mAbs showed that the V_H region of ED15 is highly acidic. Moreover, the theoretical isoelectric point of this sequence is one of the lowest p*I* values found for V_H domains in the antibody sequence database (4.3 against 6.0−8.0, Ig sequences at the NCBI database). Thus, it seems likely that the anionic character of this region could imprint a net negative charge to the ED15 paratope, making it suitable for binding the positively charged DNA-binding surface of E2. Subsequently, the ionic strength experiments allowed us to demonstrate the predominant role of the electrostatic forces in the ED15−E2C interaction. As usually observed in binding reactions between oppositely charged ligands, the association rate of the ED15−E2C interaction showed a strong dependence on ionic strength whereas the dissociation rate constant remains invariable. The k_{ass} decreases linearly as the square root of the ionic strength increases, yielding a Debye−Hückel slope value of −2.6. Notably, this value is the highest reported until now for an antibody−protein interaction (ranging from −0.5 to −1.6) (*37*−*40*).

We showed that the association of ED15 to E2C is highly sensitive to pH variations, being strongly favored at acidic pHs. Since the dimeric domain is ∼3.0 kcal mol^{-1} less stable at pH 5.6 compared to pHs above 7.0, and 6.0 kcal mol^{-1} in phosphate buffer (*15*), we believe that the pH effect is linked to the degree of stabilization of the antigen rather than to modifications in the protonation state of titrable residues at the interface. The impossibility of determining the ΔH of the ED15−E2C interaction also points out that, unlike most characterized antibody−protein complexes (*1*), the ED15−E2C is mainly entropy-driven. Although a large loss of configurational entropy upon binding would lead to a negative ΔS change, the release of water from the interface may be driving the required positive entropy change. In the same way, no reliable determinations of ΔH over a wide temperature range were observed in the thrombin−thrombomodulin interaction (*40*). Thus, despite a pending exhaustive calorimetric study of this E2C−antibody interaction, the entropic nature is clear.

Kinetic measurements at physiological salt concentrations showed that the association rate constant of this interaction is at least 1 order of magnitude slower than those generally reported in antibody−protein interactions (10^4 against 10^5−10^6 M^{-1} s^{-1}). On the other hand, the off-rate falls into the typical values, 10^{-3} to 10^{-5} s^{-1} (*38*−*41*). Considering that the ED15−E2C interaction is electrostatically steered (a factor commonly related to fast rate association constants), we would have expected the k_{ass} to be at least in the 10^5 range. However, it is important to mention that the model antigens used to characterize most classic antibody−protein interactions are compact and globular proteins of limited flexibility (e.g., lysozyme, neuraminidase) (*42*−*45*). Thus, the slow association of this complex strongly suggests that rearrangements in either or both macromolecules must take place upon complexation, posing an energy barrier. A comparison of the ED15−E2C association rate constant with that obtained for the diffusion controlled and largely electrostatically steered interaction of E2C with its target DNA sequence (10^9 M^{-1} s^{-1}) (*21*) also supports this assumption. Taken together, our present kinetic and thermodynamic experiments demonstrate that local, most likely dynamic, conformational changes on the viral domain strongly modulate the antibody affinity.

Our site-directed mutagenesis analysis showed that the epitope recognized by ED15 partially overlaps with the DNA-binding site of the transcription factor, comprising part of the recognition helix and the proximal $\beta 2$−$\beta 3$ loop. This region presents a high proportion of positively charged

residues: five basic residues in the recognition helix and two lysines (plus the potential positive charges of two histidines) in the $\beta2-\beta3$ loop. This loop is dynamic and not observable in the few HPV E2C structures available (*8*, *10*, *19*). Thus, based on the structural E2C data and in our present results, we believe that the ED15 epitope is not only highly positively charged but also remarkably flexible. This idea is in excellent agreement with the salt and pH experiments presented here. We showed that single amino acid replacements that modify the secondary structure of E2C have a dramatic effect on ED15 binding, indicating that alterations in the DNA-binding helix prevent recognition by the antibody due to alterations in the actual epitope. Despite the recent demonstration that the overall backbone conformation of E2C remains virtually unchanged upon DNA complexation, a clear differential chemical shift pattern in the recognition helix of the unbound and bound domain was pointed out (*19*). In both cases, most amide protons from the helix backbone exchange extremely fast with the solvent (*8*, *46*). Presumably, this flexibility in the DNA-contacting regions would assist the protein for reaching the most favorable DNA-complementary interface, constituting another possibility of controlling its regulatory biological functions.

Altogether, our results reveal two distinct aspects of the ED15−E2C interaction: its particularly ionic character and its entropic nature. In addition, these results illustrate the high sensitivity of this mAb to sense the conformational changes that take place on the flexible DNA-binding surface of the high risk E2 HPV16 transcription factor. The fine modulation of this antigen−antibody interaction by pH and ionic strength highlights the importance of flexibility on antibody−protein recognition and exemplify how the repertoire of the humoral immune response toward different conformers of pathogenic antigens can be expanded. Hopefully, in the next years the principles governing the recognition of more flexible regulatory proteins by specific antibodies will be addressed. Clearly these principles cannot be extracted from structures because of their dynamic nature and require the integration of thermodynamic, kinetic, and mutagenesis with structural and dynamic studies.

REFERENCES

1. Braden, B. C., and Poljak, R. J. (1995) Structural features of the reactions between antibodies and protein antigens, *FASEB J. 9*, 9−16.
2. Frauenfelder, H., Sligar, S. G., and Wolynes, P. G. (1991) The energy landscapes and motions of proteins, *Science 254*, 1598−1603.
3. Papoian, G. A., and Wolynes, P. G. (2003) The physics and bioinformatics of binding and folding-an energy landscape perspective, *Biopolymers 68*, 333−349.
4. Brown, B. M., Bowie, J. U., and Sauer, R. T. (1990) Arc repressor is tetrameric when bound to operator DNA, *Biochemistry 29*, 11189−11195.
5. Harrison, S. C., and Aggarwal, A. K. (1990) DNA recognition by proteins with the helix-turn-helix motif, *Annu. Rev. Biochem. 59*, 933−969.
6. Pabo, C. O., and Sauer, R. T. (1992) Transcription factors: structural families and principles of DNA recognition, *Annu. Rev. Biochem. 61*, 1053−1095.
7. Spolar, R. S., and Record, M. T., Jr. (1994) Coupling of local folding to site-specific binding of proteins to DNA, *Science 263*, 777−784.
8. Liang, H., Petros, A. M., Meadows, R. P., Yoon, H. S., Egan, D. A., Walter, K., Holzman, T. F., Robins, T., and Fesik, S. W. (1996) Solution structure of the DNA-binding domain of a human papillomavirus E2 protein: evidence for flexible DNA-binding regions, *Biochemistry 35*, 2095−2103.
9. Lima, L. M., and Prat-Gay, G. de. (1997) Conformational changes and stabilization induced by ligand binding in the DNA-binding domain of the E2 protein from human papillomavirus, *J. Biol. Chem. 272*, 19295−19303.
10. Nadra, A. D., Eliseo, T., Mok, Y. K., Almeida, C. L., Bycroft, M., Paci, M., Prat-Gay, G. de., and Cicero, D. O. (2004) Solution structure of the HPV-16 E2 DNA binding domain, a transcriptional regulator with a dimeric beta-barrel fold, *J. Biomol. NMR 30*, 211−214.
11. Hegde, R. S. (2002) The papillomavirus E2 proteins: structure, function, and biology, *Annu. Rev. Biophys. Biomol. Struct. 31*, 343−360.
12. McBride, A. A., Romanczuk, H., and Howley, P. M. (1991) The papillomavirus E2 regulatory proteins, *J. Biol. Chem. 266*, 18411−18414.
13. Hegde, R. S., Grossman, S. R., Laimins, L. A., and Sigler, P. B. (1992) Crystal structure at 1.7 A of the bovine papillomavirus-1 E2 DNA-binding domain bound to its DNA target, *Nature 359*, 505−512.
14. Hegde, R. S., and Androphy, E. J. (1998) Crystal structure of the E2 DNA-binding domain from human papillomavirus type 16: implications for its DNA binding-site selection mechanism, *J. Mol. Biol. 284*, 1479−1489.
15. Mok, Y. K., Prat-Gay, G. de., Butler, P. J., and Bycroft, M. (1996) Equilibrium dissociation and unfolding of the dimeric human papillomavirus strain-16 E2 DNA-binding domain, *Protein Sci. 5*, 310−319.
16. Mok, Y. K., Bycroft, M., and Prat-Gay, G. de. (1996) The dimeric DNA binding domain of the human papillomavirus E2 protein folds through a monomeric intermediate which cannot be native-like, *Nat. Struct. Biol. 3*, 711−717.
17. Prat-Gay, G. de., Nadra, A. D., Corrales-Izquierdo, F. J., Alonso, L. G., Ferreiro, D. U., and Mok, Y. K. (2005) The folding mechanism of a dimeric beta-barrel domain, *J. Mol. Biol. 351*, 672−682.
18. Mok, Y. K., Alonso, L. G., Lima, L. M., Bycroft, M., and Prat-Gay, G. de. (2000) Folding of a dimeric beta-barrel: residual structure in the urea denatured state of the human papillomavirus E2 DNA binding domain, *Protein Sci. 9*, 799−811.
19. Cicero, D. O., Nadra, A. D., Eliseo, T., Dellarole, M., Paci, M., and Prat-Gay, G. de. (2006) Structural and Thermodynamic Basis for the Enhanced Transcriptional Control by the Human Papillomavirus Strain-16 E2 Protein, *Biochemistry 45*, 6551−6560.
20. Lima, L. M., Foguel, D., and Silva, J. L. (2000) DNA tightens the dimeric DNA-binding domain of human papillomavirus E2 protein without changes in volume, *Proc. Natl. Acad. Sci. U.S.A. 97*, 14289−14294.
21. Ferreiro, D. U., and Prat-Gay, G. de. (2003) A protein-DNA binding mechanism proceeds through multi-state or two-state parallel pathways, *J. Mol. Biol. 331*, 89−99.
22. Cerutti, M. L., Centeno, J. M., Prat-Gay, G. de., and Goldbaum, F. A. (2003) Antibody response to a viral transcriptional regulator, *FEBS Lett. 534*, 202−206.
23. Ferreiro, D. U., Lima, L. M., Nadra, A. D., Alonso, L. G., Goldbaum, F. A., and Prat-Gay, G. de. (2000) Distinctive cognate sequence discrimination, bound DNA conformation, and binding modes in the E2 C-terminal domains from prototype human and bovine papillomaviruses, *Biochemistry 39*, 14692−14701.
24. Harper, M., Lema, F., Boulot, G., and Poljak, R. J. (1987) Antigen specificity and cross-reactivity of monoclonal anti-lysozyme antibodies, *Mol. Immunol. 24*, 97−108.
25. Orlandi, R., Gussow, D. H., Jones, P. T., and Winter, G. (1989) Cloning immunoglobulin variable domains for expression by the polymerase chain reaction, *Proc. Natl. Acad. Sci. U.S.A. 86*, 3833−3837.
26. Kabat, E. A., Wu, T. T., Reid-Miller, M., Perry, H. M., and Gottesman, K. S. (1987) *Sequences of proteins of immunological interest*, Public Health Service, National Institutes of Health.
27. Chothia, C., and Lesk, A. M. (1987) Canonical structures for the hypervariable regions of immunoglobulins, *J. Mol. Biol. 196*, 901−917.
28. Gasteiger, E., Hoogland, C., Gattiker, A., Duvaud, S., Wilkins, M. R., Appel, R. D., and Bairoch, A. (2005) Protein identification and analysis tools on the ExPASy Server, in *The Proteomics*

Protocols Handbook (Walker, J. M., Ed.) pp 571−607, Humana Press, Totowa, NJ.
29. Baerga-Ortiz, A., Rezaie, A. R., and Komives, E. A. (2000) Electrostatic dependence of the thrombin-thrombomodulin interaction, *J. Mol. Biol. 296*, 651−658.
30. Ferreiro, D. U., Dellarole, M., Nadra, A. D., and de Prat-Gay, G. (2005) Free energy contributions to direct readout of a DNA sequence, *J. Biol. Chem. 280*, 32480−32484.
31. Foote, J., and Milstein, C. (1994) Conformational isomerism and the diversity of antibodies, *Proc. Natl. Acad. Sci. U.S.A. 91*, 10370−10374.
32. Jimenez, R., Salazar, G., Baldridge, K. K., and Romesberg, F. E. (2003) Flexibility and molecular recognition in the immune system, *Proc. Natl. Acad. Sci. U.S.A. 100*, 92−97.
33. James, L. C., Roversi, P., and Tawfik, D. S. (2003) Antibody multispecificity mediated by conformational diversity, *Science 299*, 1362−1367.
34. James, L. C., and Tawfik, D. S. (2005) Structure and kinetics of a transient antibody binding intermediate reveal a kinetic discrimination mechanism in antigen recognition, *Proc. Natl. Acad. Sci. U.S.A. 102*, 12730−12735.
35. Manivel, V., Sahoo, N. C., Salunke, D. M., and Rao, K. V. (2000) Maturation of an antibody response is governed by modulations in flexibility of the antigen-combining site, *Immunity 13*, 611−620.
36. Nair, D. T., Singh, K., Siddiqui, Z., Nayak, B. P., Rao, K. V., and Salunke, D. M. (2002) Epitope recognition by diverse antibodies suggests conformational convergence in an antibody response, *J. Immunol. 168*, 2371−2382.
37. Xavier, K. A., McDonald, S. M., McCammon, J. A., and Willson, R. C. (1999) Association and dissociation kinetics of bobwhite quail lysozyme with monoclonal antibody HyHEL-5, *Protein Eng. 12*, 79−83.
38. Xavier, K. A., and Willson, R. C. (1998) Association and dissociation kinetics of anti-hen egg lysozyme monoclonal antibodies HyHEL-5 and HyHEL-10, *Biophys. J. 74*, 2036−2045.
39. Raman, C. S., Jemmerson, R., Nall, B. T., and Allen, M. J. (1992) Diffusion-limited rates for monoclonal antibody binding to cytochrome c, *Biochemistry 31*, 10370−10379.
40. Baerga-Ortiz, A., Bergqvist, S., Mandell, J. G., and Komives, E. A. (2004) Two different proteins that compete for binding to thrombin have opposite kinetic and thermodynamic profiles, *Protein Sci. 13*, 166−176.
41. Goldbaum, F. A., Cauerhff, A., Velikovsky, A., Llera, A. S., Riottot, M. M., and Poljak, R. J. (1999) Lack of significant differences in association rates and affinities of antibodies from short-term and long-term responses to hen egg lysozyme, *J. Immunol. 162*, 6040−6045.
42. Kunichika, K., Hashimoto, Y., and Imoto, T. (2002) Robustness of hen lysozyme monitored by random mutations, *Protein Eng. 15*, 805−809.
43. Li, Y., Li, H., Yang, F., Smith-Gill, S. J., and Mariuzza, R. A. (2003) X-ray snapshots of the maturation of an antibody response to a protein antigen, *Nat. Struct. Biol. 10*, 482−488.
44. Cauerhff, A., Goldbaum, F. A., and Braden, B. C. (2004) Structural mechanism for affinity maturation of an anti-lysozyme antibody, *Proc. Natl. Acad. Sci. U.S.A. 101*, 3539−3544.
45. Colman, P. M., and Smith, B. J. (2003) Specificity and Promiscuity in Protein-Ligand and Protein-Protein Interactions, *Aust. J. Chem. 56*, 763−767.
46. Nadra, A. D. (2006) Ph.D. Thesis, Universidad de Buenos Aires.
47. Humphrey, W., Dalke, A., and Schulten, K. (1996) VMD: visual molecular dynamics, *J. Mol. Graphics 14*, 33−38, 27−38.

BI0615184